

Supporting information for

Efficient lignin conversion over Ni/(Fe/Zn/Co/Mo/Cu)-WO₃/Al₂O₃ for selectively
yielding alkyl phenols

Xinyu Lu, Xiaoli Gu*

Jiangsu Co-Innovation Center of Efficient Processing and Utilization of Forest Resources, Jiangsu Provincial
Key Lab for the Chemistry and Utilization of Agro-forest biomass, College of Chemical Engineering, Nanjing
Forestry University, Nanjing 210037, China.

*Corresponding authors: guxiaoli@njfu.edu.cn

Figures

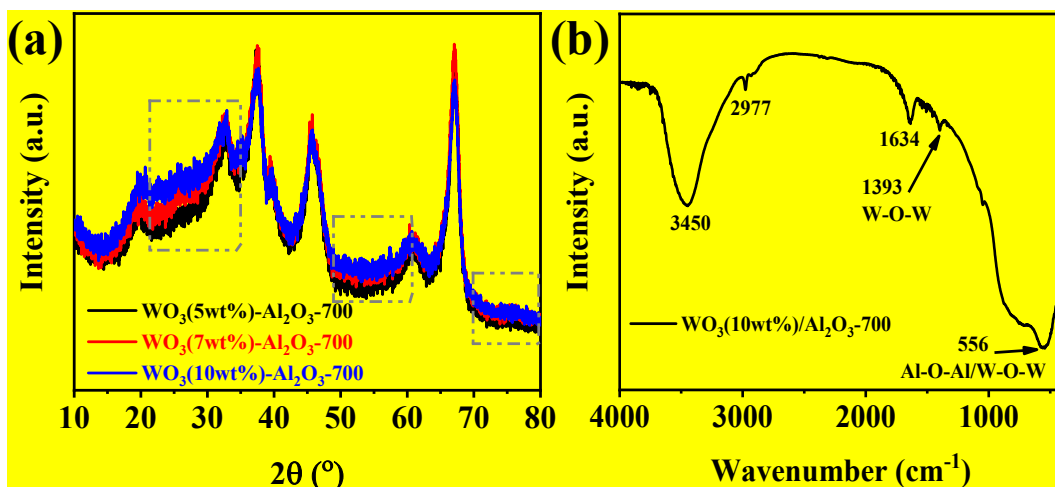
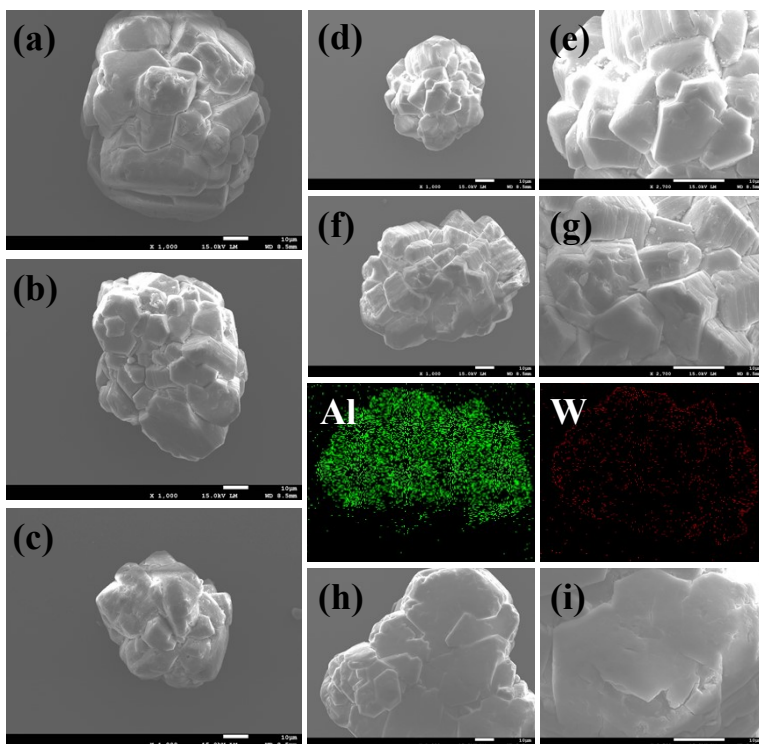


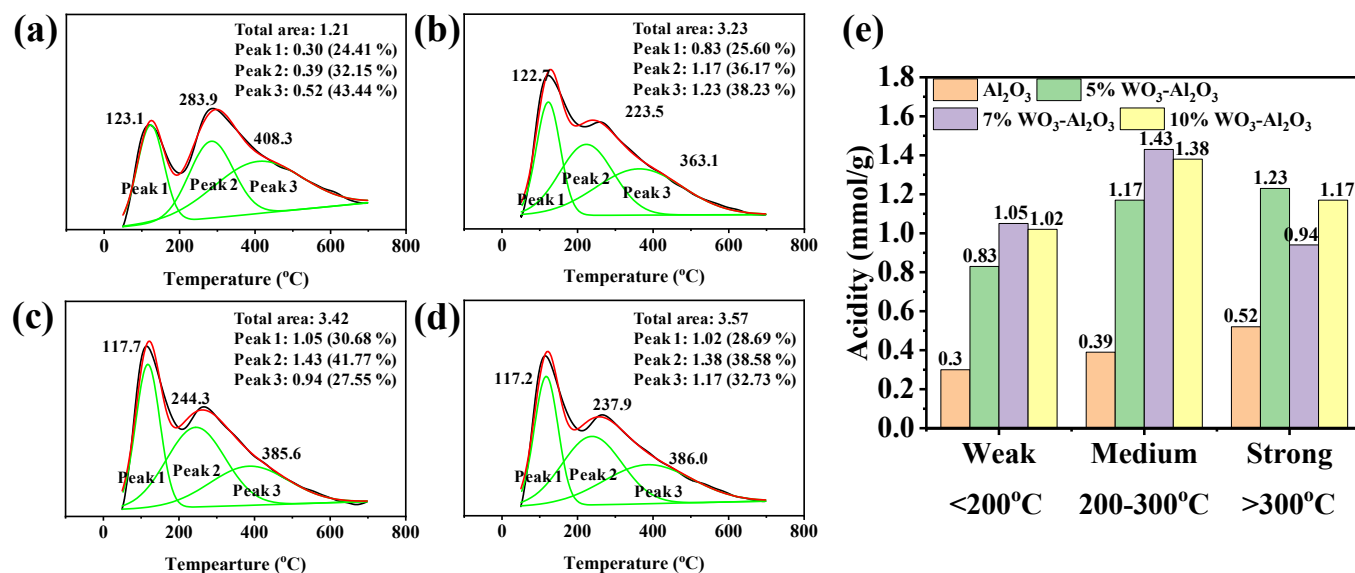
Fig. S1. (a) XRD patterns and (b) FTIR spectrum of tungsten modified supports.



14

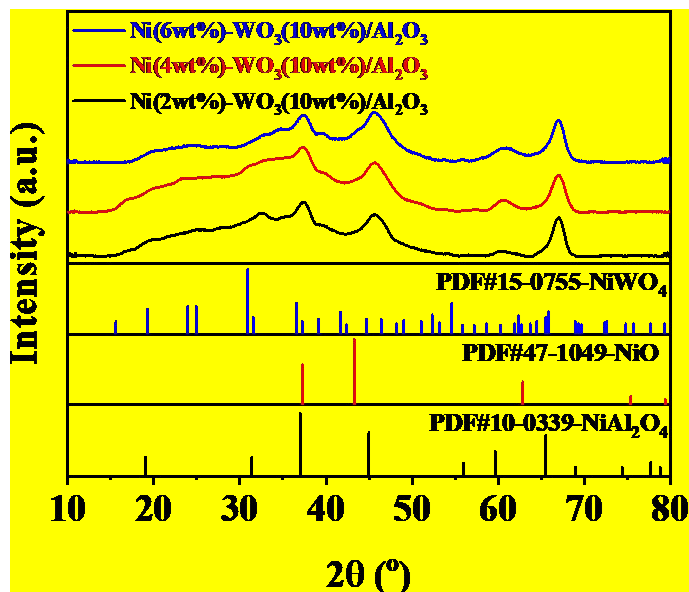
15 **Fig. S2.** SEM images of parent Al_2O_3 after calcination at (a) 500 °C, (b) 700 °C and (c) 900 °C. SEM images of
 16 $\text{WO}_3(10\text{wt}\%)/\text{Al}_2\text{O}_3$ under low magnification (d: at 500 °C; f: at 700 °C; h: at 900 °C) and high magnification (e:
 17 at 500 °C; g: at 700 °C; i: at 900 °C), and EDS analysis (alumina and tungsten elements) of $\text{WO}_3(10\text{wt}\%)/\text{Al}_2\text{O}_3$
 18 prepared at 700 °C.

19



20

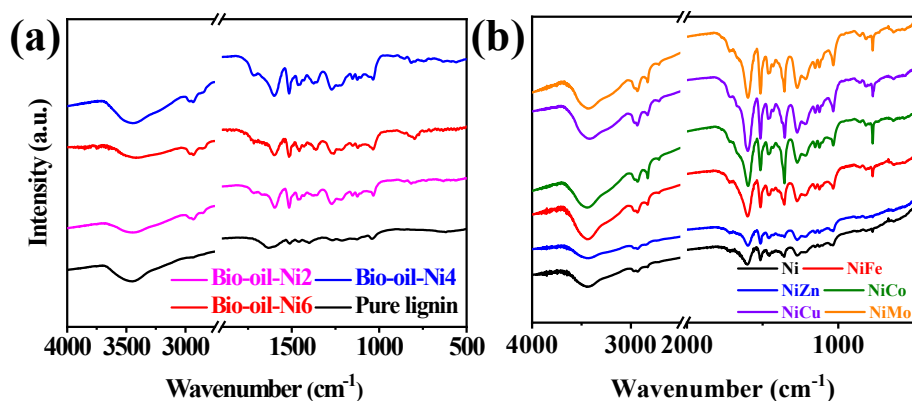
21 **Fig. S3.** (a-d) Peak fitting results of NH_3 -TPD (a: Al_2O_3 -700; b: $\text{WO}_3(5\text{wt}\%)/\text{Al}_2\text{O}_3$ -700; c: $\text{WO}_3(7\text{wt}\%)/\text{Al}_2\text{O}_3$ -
 22 700; d: $\text{WO}_3(10\text{wt}\%)/\text{Al}_2\text{O}_3$ -700), and (e) their acidity contributions.



23

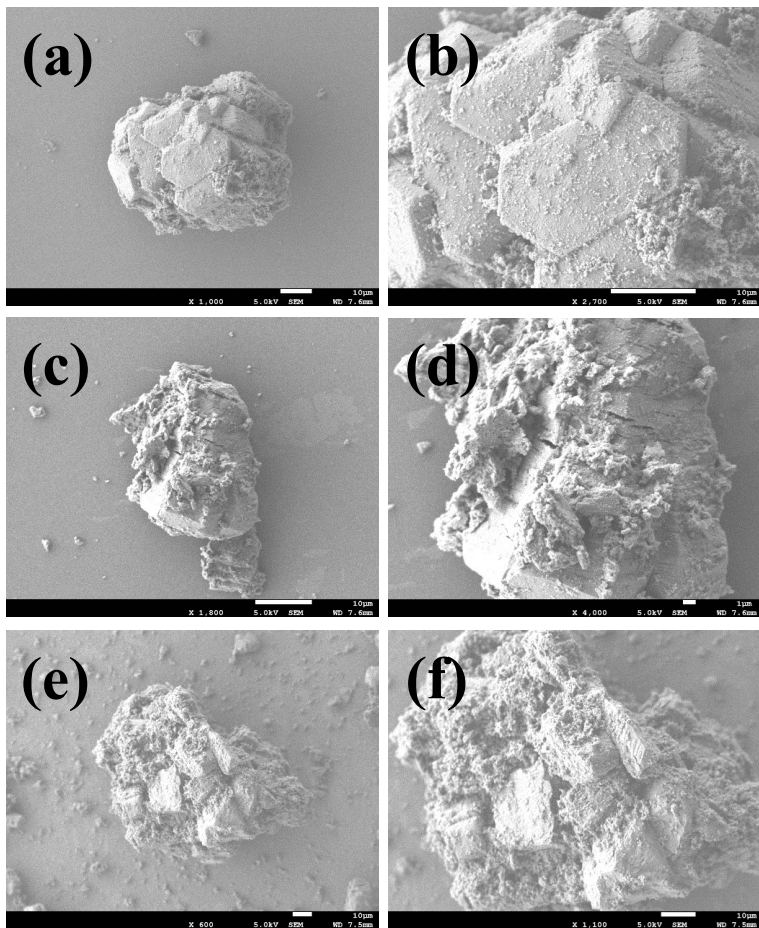
24 **Fig. S4.** XRD spectra of Ni-WO₃(10wt%)/Al₂O₃ with different Ni loading.

25



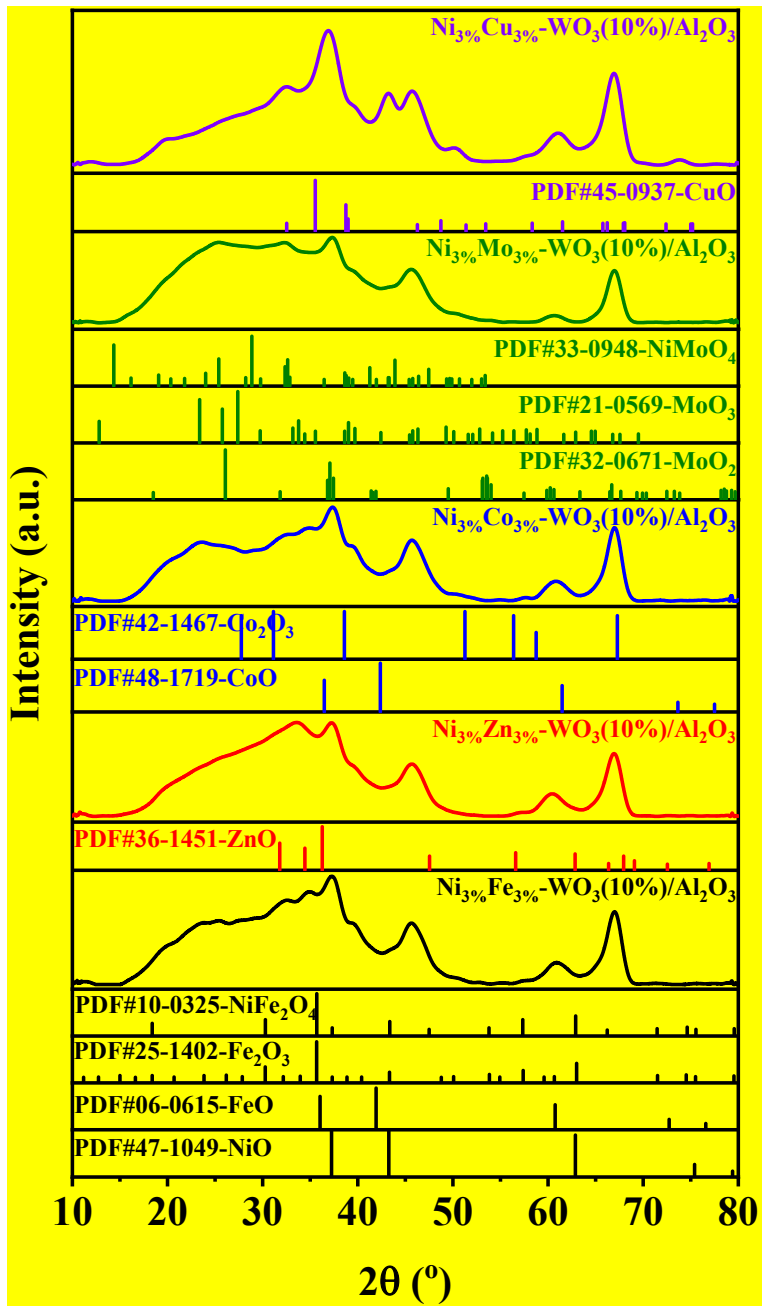
26

27 **Fig. S5.** FTIR spectra of lignin-derived bio-oils obtained from lignin depolymerization at (a) Ni(4~6wt%)-
 28 WO₃(10wt%)/Al₂O₃-700, and (b) Ni_{3wt%}-X_{3wt%}/WO₃(10wt%)/Al₂O₃-700 (X = Fe/Zn/Co/Mo/Cu).



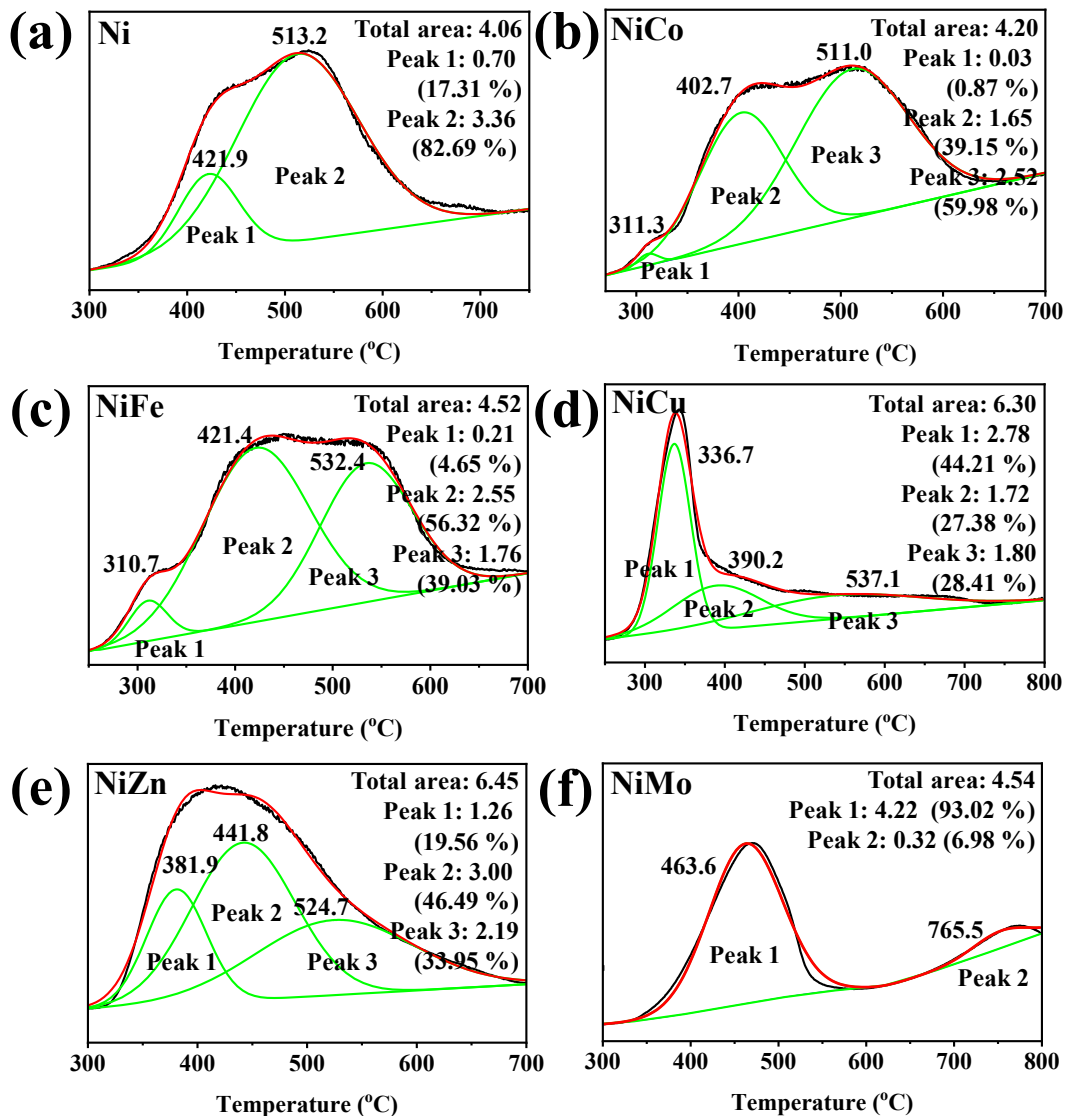
29

30 **Fig. S6.** SEM images of Ni(4 ~ 6 wt%)-WO₃(10 wt%)/Al₂O₃-700 under low magnification (a: 2 wt% Ni loading;
31 c: 4 wt% Ni loading; e: 6 wt% Ni loading) and high magnification (b: 2 wt% Ni loading, d: 4 wt% Ni loading, f:
32 6 wt% Ni loading).



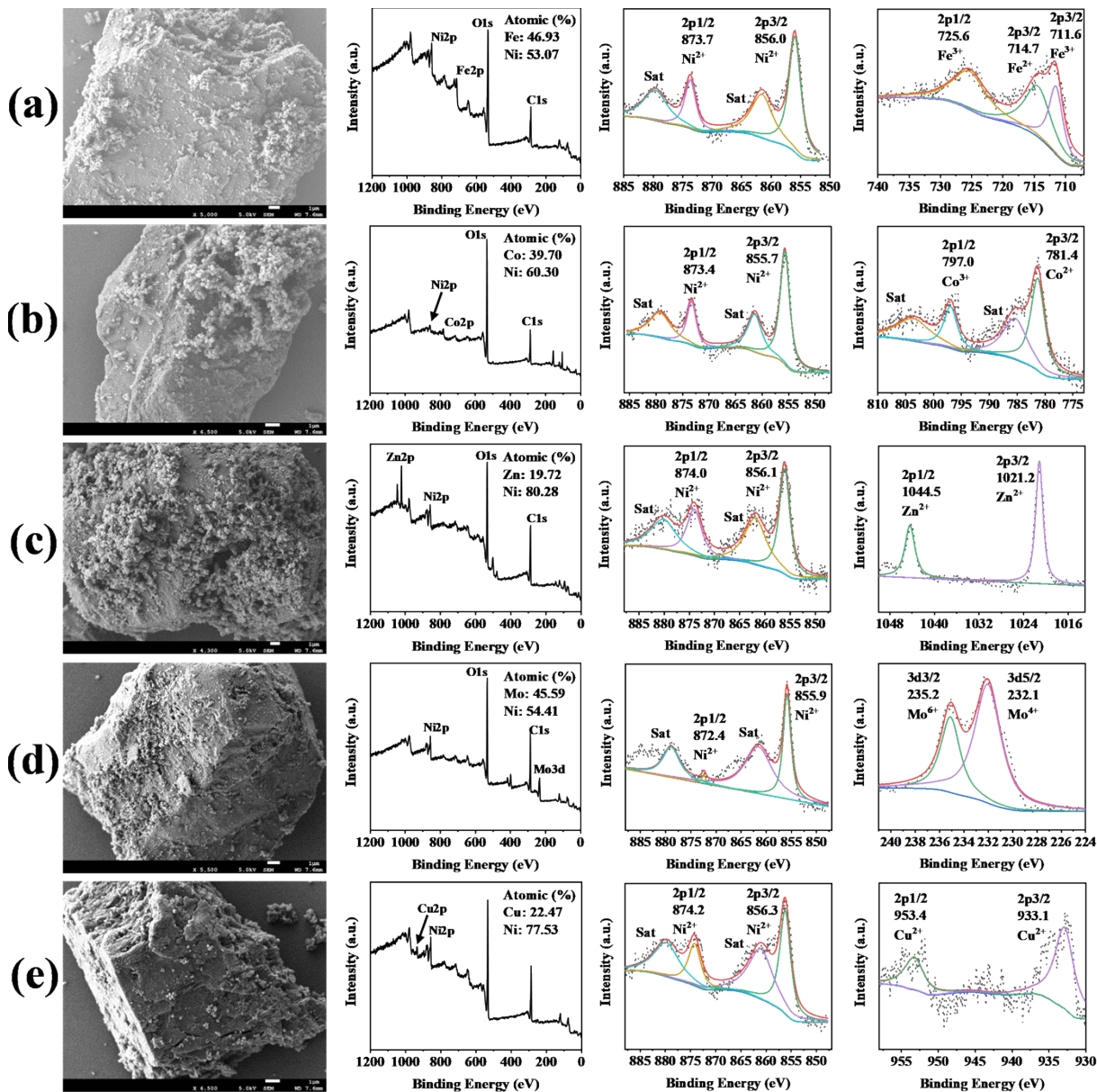
33

34 **Fig. S7.** XRD spectra of $\text{Ni}_{3\text{wt}\%}\text{-X}_{3\text{wt}\%}/\text{WO}_3(10\text{wt}\%)/\text{Al}_2\text{O}_3\text{-700}$ ($X = \text{Fe}/\text{Zn}/\text{Co}/\text{Mo}/\text{Cu}$).



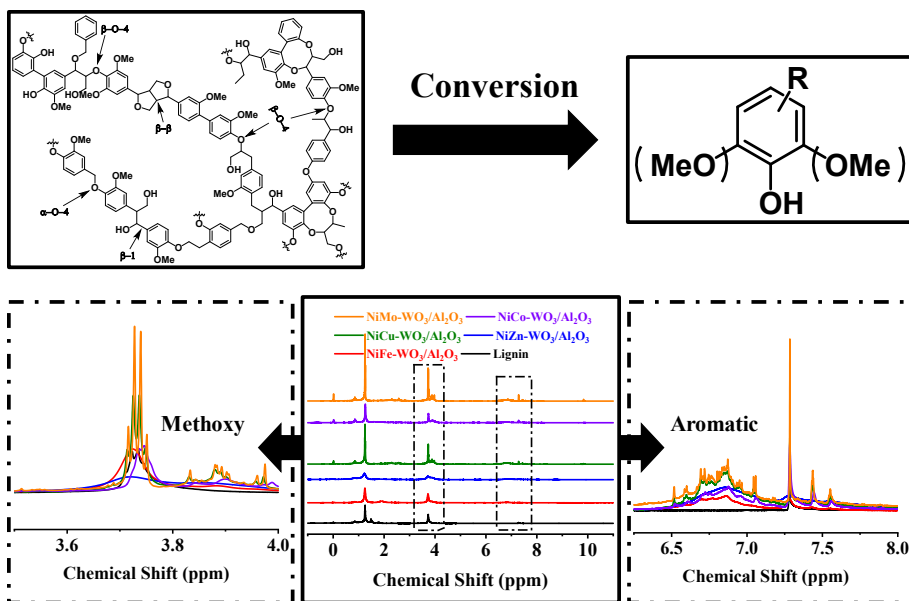
35

36 **Fig. S8.** Peak fitting results of H₂-TPR of single and bimetallic Ni-based catalysts.



37

38 **Fig. S9.** SEM images and XPS spectra of Ni_{3wt%}-X_{3wt%}/WO₃(10wt%)/Al₂O₃-700 (X = (a) Fe/(b) Zn/(c) Co/(d)
 39 Mo/(e) Cu).



40

41 **Fig. S10.** ^1H NMR spectra of bio-oils obtained from lignin degradation at Ni(3wt%)-X(3wt%,
 42 Fe/Zn/Co/Mo/Cu)/WO₃(10wt%)/Al₂O₃-700.

43

44 **Tables**

45 **Table S1.** Elemental analysis of lignin.

C (wt%)	H (wt%)	N (wt%)	O ^a (wt%)	H:C ^b	O:C ^b
61.85	6.87	0.15	31.13	1.33	0.38

46 ^a Determined via residual mass balance.

47 ^b Molar ratio.

48

49 **Table S2.** Quantitative analysis of representative phenolic compounds in bio-oils.

Compounds (wt%)	Ni/Fe	Ni/Zn	Ni/Co	Ni/Mo	Ni/Cu
2-Methoxy-phenol	0.9	2.4	0.6	0.9	0.6
Vanillin	2.8	0.7	0.7	2.3	2.6
Homovanillyl alcohol	0.5	0.7	2.9	1.1	0.9

50